International Journal of Nanomedicine

Dovepress
Taylor & Francis Group

Open Access Full Text Article

ORIGINAL RESEARCH

Combination of Ketorolac Tromethamine and Prednisolone-Loaded PLGA Nanocomposite for Effective Chronic Pain Relief in Mice

Tuyet-Nhi Do[1], Yen-Chin Liu[2–4], Yu-Che Chuang[5], Tsung-Lin Tsai[1,6,7], Ping-Ching Wu[1,6,8–10]

[1]Department of Biomedical Engineering, College of Engineering, National Cheng Kung University, Tainan, 701, Taiwan; [2]School of Post-Baccalaureate, College of Medicine, Kaohsiung Medical University, Kaohsiung, 812, Taiwan; [3]Department of Anesthesiology, Kaohsiung Municipal Siaogang Hospital, Kaohsiung Medical University Hospital, Kaohsiung Medical University, Kaohsiung, 812, Taiwan; [4]Department of Anesthesiology, National Cheng Kung University Hospital, College of Medicine, National Cheng Kung University, Tainan, 701, Taiwan; [5]Department of Pathology and Laboratory Medicine, Taipei Veterans General Hospital, Taipei, 112, Taiwan; [6]Center of Applied Nanomedicine, National Cheng Kung University, Tainan, 701, Taiwan; [7]Department of Oncology, National Cheng Kung University Hospital, College of Medicine, National Cheng Kung University, Tainan, 701, Taiwan; [8]Institute of Oral Medicine and Department of Stomatology, National Cheng Kung University Hospital, College of Medicine, National Cheng Kung University, Tainan, 701, Taiwan; [9]Medical Device Innovation Center, Taiwan Innovation Center of Medical Devices and Technology, National Cheng Kung University Hospital, National Cheng Kung University, Tainan, 701, Taiwan; [10]University Center of Bioscience and Biotechnology, National Cheng Kung University, Tainan, 701, Taiwan

Correspondence: Ping-Ching Wu, Department of Biomedical Engineering, National Cheng Kung University, Tainan, 701, Taiwan, Email wbcxyz@gmail.com; Tsung-Lin Tsai, Department of Oncology, National Cheng Kung University Hospital, College of Medicine, National Cheng Kung University, Tainan, 701, Taiwan, Email sloantsai@mail.ncku.edu.tw

Introduction: Chronic pain is a complex condition that requires timely and effective management to prevent long-term emotional, social, and economic consequences. This study aims to develop a poly(lactic-co-glycolic acid) (PLGA)-based nanocomposite co-loaded with ketorolac tromethamine (KT) and prednisolone (PRED) to improve therapeutic efficacy and reduce systemic side effects associated with conventional treatments.

Methods: KT-PRED-PLGA nanoparticles were synthesized via a double emulsion method and characterized for their physicochemical properties and biocompatibility. A chronic inflammatory pain model was established in ICR mice using Complete Freund's Adjuvant (CFA). Mechanical pain thresholds were evaluated using Dixon's up-and-down method. Histopathological and immunohistochemical analyses were performed to evaluate systemic toxicity and inflammation-related protein expression.

Results: The KT-PRED-PLGA nanoparticles exhibited favorable characteristics, including a mean particle size of 166.2 ± 8.0 nm, a polydispersity index of 0.14, a zeta potential of −15.8 ± 0.3 mV, and encapsulation efficiency exceeding 80%. The nanoparticles sustained drug release up to 92.5% over 120 h. In vitro assays demonstrated the KT-PRED-PLGA nanoparticles revealed high biocompatibility in Vero cells after 72 h of exposure. In vivo experiments demonstrated significantly reduced pain behaviors and tissue inflammation, with minimal toxicity. Behavioral assessments confirmed enhanced analgesic and anti-allodynic effects over the free drugs. Reduced expression of cyclooxygenases (COX-1 and COX-2) and prostaglandin E_2 (PGE_2) in hind paw tissues confirmed improved anti-inflammatory activity.

Conclusion: KT-PRED-PLGA nanoparticles offer safe, sustained analgesia with enhanced therapeutic efficacy and reduced systemic toxicity, highlighting their strong potential for future clinical translation in chronic pain therapy.

Keywords: ketorolac tromethamine and prednisolone encapsulation, PLGA nanoparticle drug delivery, nanomedicine, double emulsion strategy, chronic inflammatory pain relief

Introduction

Pain is a sensation of discomfort associated with tissues, including acute and chronic pain. Trauma or internal diseases typically cause acute pain, a type of intense pain that lasts for a short period.[1] It typically manifests within less than four weeks and subsides once the wound heals. Chronic pain lasts longer than acute, usually up to 3–6 months, and can be mild, dull, or intense pain of any cause.[2] Pain is conceptualized as a pathological state requiring prompt intervention to

Received: 17 January 2025
Accepted: 9 June 2025
Published: 27 June 2025

Graphical Abstract

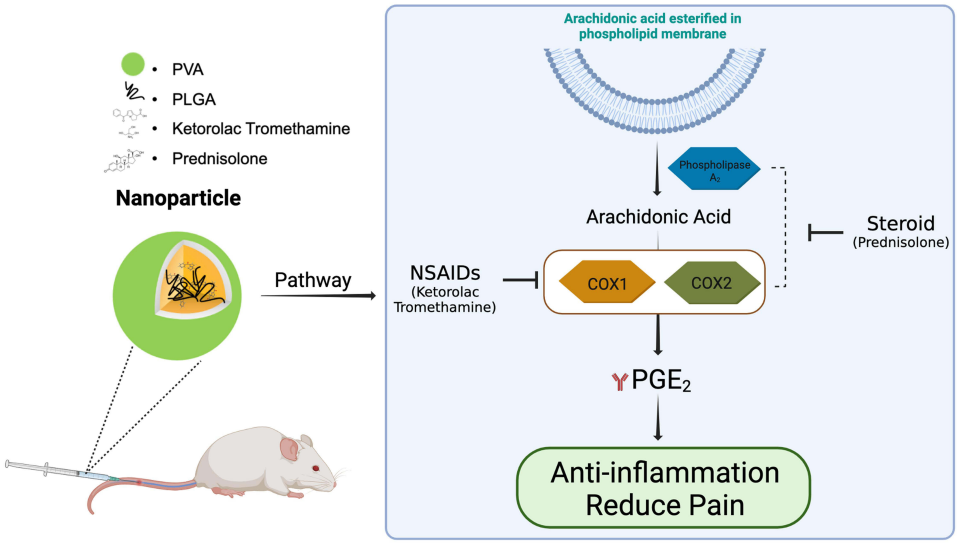

prevent consequences that extend beyond individual suffering to encompass familial and societal ramifications.[2,3] These ramifications are multifaceted, encompassing emotional, economic, and social dimensions. The American Society of Anesthesiologists (ASA) published this burden status for approximately 60 million people, with at least 10% of the world's population suffering from chronic pain. The estimation rates are nearly 20–25% in some countries and regions.[1,2] Optimal medicine, high pain relief, safety, and low degradability are still needed to avoid waste and save on the budget.[4]

Therefore, we wanted to profoundly investigate the role of "chronic pain relief" with the best efficiency and safety. The prevailing clinical analgesics are commonly categorized into potent opioids and nonsteroidal anti-inflammatory drugs (NSAIDs).[4–6] Relevant investigations have shown that ketorolac tromethamine (KT), an NSAID, is highly effective for managing moderate to severe pain, often outperforming other analgesics and even rivaling narcotic options.[7,8] Prednisolone (PRED) a type of corticosteroid, reduces inflammation by addressing swelling and allergic reactions.[9,10] KT and PRED offer a synergistic approach to treating pain and inflammation, making them ideal for dual therapy.[11,12] Previous studies using KT 0.5% and PRED acetate 1% solutions have demonstrated limited clinical performance due to rapid systemic clearance, short half-life, and frequent dosing requirements. These conventional free drugs are also associated with severe gastrointestinal and renal side effects when administered systemically.[13,14] Conversely, PLGA-based co-encapsulation offers a sustained and controlled drug release profile, potentially enhancing therapeutic efficacy while reducing dosing frequency and minimizing adverse effects.[15,16] Encapsulating KT and PRED within poly (lactic-co-glycolic acid) (PLGA) nanoparticles addresses limitations such as rapid clearance and low bioavailability, allowing controlled, sustained drug release (DR).[17–19] This double emulsion ensures prolonged therapeutic effects, improved stability, and targeted delivery, reducing side effects. Incorporating hydrophilic KT and hydrophobic PRED into a single system is the most challenging aspect. Therefore, precise optimization of the double emulsion process is essential to achieve high drug loading (DL), encapsulation efficiency (EE), stable DR, and consistent drug stability.[3,20] The development of novel pharmacological treatment methods with enduring efficacy and minimal adverse effects remains a principal challenge in /investigating chronic inflammatory pain. However, this challenge has been addressed through the advancement of single-step water-in-oil-in-water (W/O/W) synthesis methods for PLGA nanoparticles.[11,18,21] This innovation originates from the development of systematic W/O/W synthesis approaches for PLGA nanoparticles. These nanoparticles enable the concurrent encapsulation of the hydrophilic NSAID KT and the hydrophobic corticosteroid PRED, yielding a dual-encapsulation strategy.[22] By utilizing these nanocarriers, the nanocarriers promote compatibility, contribute to the effectiveness of long-term treatment, and diminish adverse effects, including several severe complications associated with KT therapy such as liver and/or acute renal failure, gastrointestinal ulceration, postoperative

bleeding, perforation, and anaphylactic and anaphylactoid reactions.[22,23] Furthermore, integrating a one-step synthesis approach for PLGA with a corticosteroid (specifically, the hydrophobic drug PRED) extends the uptake period, thereby optimizing the management of chronic inflammatory pain.[24,25] Given these limitations of conventional free drugs, we hypothesized that dual-drug-loaded PLGA nanoparticles would provide synergistic analgesic and anti-inflammatory effects with improved pharmacokinetics and safety in chronic inflammatory pain models.

Our research aimed to amalgamate double emulsification nanocarriers to offer a synergistic therapeutic combination and facilitate dosage reduction, attenuation of side effects, and cost-effectiveness in treatment. A novel strategy for pain relief in this study, involving the development of dual drug-encapsulated PLGA nanoparticles. Different dosages were administered to assess the effectiveness of the analgesic treatment, and the expression levels of COX-1, COX-2,[6,26,27] and PGE_2[28] were evaluated to confirm the reliability of the pain relief pathway.

Materials and Methods

Poly(lactic-co-glycolic acid) 50:50 (PLGA, Evonik); poly(vinyl alcohol) (PVA, Sigma–Aldrich); ketorolac tromethamine (KT, 042412, Yungshin Co., Taichung City, Taiwan); prednisolone (PRED, Sigma–Aldrich); dichloromethane (DCM, J.T. Baker); ethyl acetate (EtAc, Macron); dimethyl sulfoxide (DMSO, Sigma–Aldrich); 99.9% ethanol (EtOH, Sigma–Aldrich); xylenes (Sigma–Aldrich); Tween 20 (Sigma–Aldrich); 10× Phosphate-buffered saline (PBS, TissuePro); high glucose Dulbecco's Modified Eagle's Medium (HG-DMEM, Gibco); sodium bicarbonate (Sigma–Aldrich); cell counting kit-8 (CCK-8 kit, Dojindo); paraformaldehyde (PFA, Sigma–Aldrich); fetal bovine serum (FBS, Gibco); trypsin-EDTA solution (Caisson Labs); antibiotics and antimycotics (GeneDireX); hydrochloric acid (HCl, Sigma–Aldrich); hematoxylin and eosin (H&E, Leica); isoflurane (USP, Halocarbon); Complete Freund's Adjuvant (CFA, Sigma–Aldrich); 3,3′-diaminobenzidine (DAB, Vector SK-4100); hematoxylin solution (Mayer's, modified); anti-cyclooxygenase 1 (COX-1, ab133319, Abcam, Cambridge, MA, USA); anti-cyclooxygenase 2 (COX-2, ab15191, Abcam, Cambridge, UK); rabbit anti-prostaglandin E_2 polyclonal antibody (PGE_2, Bioss Inc., Woburn, MA, USA).

Preparation of KT-PRED-PLGA Nanoparticles via Dual Emulsion Encapsulation

A dual-encapsulated painkiller was formulated by encapsulating hydrophilic KT and hydrophobic PRED within PLGA nanoparticles in a pain model. The process was thorough, beginning with the addition of 1 mL of KT (30 mg/mL) and 30 mg of PLGA (50:50 DLG 4.5A) to 2.5 mL of EtAc in an ice bath and sonication at 60% amplitude for 2 min via a VCX 130 Ultrasonic Processor. Next, 30 mg of PRED and 100 mg of PLGA in 2.5 mL of DCM were mixed with the KT/PLGA solution, followed by a second round of sonication for 2 min at 60% amplitude.[29] The mixture was then combined with 10 mL of a 1% w/v PVA stabilizer and sonicated again. After sonication, the mixture was transferred to a two-neck bottle, where it was subjected to constant stirring at 400 rpm in a water container heated to 80 °C to facilitate diffusion and remove the organic solvents. Using a vacuum system at this stage was critical to ensure the complete removal of the organic solvents and promote the reaction.[29,30] Finally, the remaining free drugs and PVA were removed by ultracentrifugation at 12,000 rpm for 15 min at 4 °C. The resulting KT-PRED-PLGA nanoparticles, a product of the entire process, were washed three times with deionized water and then stored in deionized water at 4 °C.

Determination of Drug Encapsulation Efficiency and Size Characterization of KT-PRED-PLGA Nanoparticles

The nanocapsules were comprehensively analyzed via UV-VIS spectrophotometry with a Thermo Scientific NanoDropOne microvolume instrument. UV absorption was measured at 248 nm and 325 nm for PRED and KT. The EE percentage (%EE) was calculated by dividing the weight of drugs encapsulated in the KT-PRED-PLGA nanoparticles by the initial weight of the drug used. The DL percentage (%DL) was determined by dividing the weight of the drugs in the KT-PRED-PLGA nanoparticles by the total weight of the nanoparticles.[21,31]

Equation 1. The formula for %EE:

$$\%EE = \frac{\text{Weight of drug in nanoparticles}}{\text{Weight of the feeding drug}} \times 100$$

https://doi.org/10.2147/IJN.S515452

Equation 2. The formula for %DL:

$$\%DL = \frac{\text{Weight of drug in nanoparticles}}{\text{Weight of nanoparticles}} \times 100$$

The mean particle size (hydrodynamic diameter) was determined via thoroughness via dynamic light scattering (DLS) after diluting the nanocapsule suspension (1:100, v/v) in deionized water, which was measured with a Delsa Nano (Beckman Coulter) at 25 °C. The size distribution and polydispersity were reported as the mean of three determinations performed in triplicate. The value of the zeta potential was determined with the zeta potential (Beckman Coulter Delsa Nano instrument). Analyses were performed by diluting the nanocapsule suspension in deionized water (1:100, v/v), and the results were expressed in three replicates. We used the JEM-1400 Transmission Electron Microscope (TEM, JEOL, USA) technique to analyze the shape of the PLGA, KT-PLGA, and KT-PRED-PLGA nanoparticles.[32] The samples were dissolved completely and diluted with deionized water, and then placed onto a mesh made of copper, after which negative staining was performed. After that, the examination will be conducted using the solutions 15k and 60k.

Vitro Drug Release Study of KT-PRED-PLGA Nanoparticles

In vitro drug diffusion experiments were performed via the dialysis bag technique.[17] Drug-loaded nanoparticles (5 mL) were dispersed within the dialysis bags, which were subsequently immersed in a glass screw-capped bottle filled with 35 mL of pH 8.5 hG-DEMEM and 20% FBS.[33] The bottle was maintained at 37 ± 1°C with a magnetic stirrer and constant agitation throughout the experiment. During the whole of the experiment, the speed of the stir bar was maintained at 100 rpm. Samples (0.1 mL) were withdrawn and substituted at predetermined time points with equal volumes of freshly prepared pH 8.5 hG-DMEM.[17,32] Following appropriate dilution, the samples were thoroughly analyzed via a UV-Vis spectrophotometer at 325 nm for KT and 248 nm for PRED, ensuring the validity of our results. The DR percentage (%DR) was calculated as the weight of drug release divided by the weight of drugs in nanoparticles through cumulative time.

Equation 3. The formula for %DR:

$$\%DR = \frac{\text{Weight of drug release}}{\text{Weight of drug in nanoparticles}} \times 100$$

Assessment of Cell Cytotoxicity Using CCK-8

Free drugs and nanoparticles have been assessed for toxicity through in vitro tests on Vero cell lines (ATCC-CCL-81). The cells were cultured under physiological conditions in an incubator (37 °C, 5% CO_2, 95% relative humidity). Vero cells were harvested and cultured in 96-well plates with 5000 cells in each well.[34,35] Different treatments were added, including HG-DMEM supplemented with 10% FBS, free drugs, and nanoparticles at various concentrations (100 µL/well). The number of viable cells in a population was measured at continuous retention times of 1 h, 3 h, 6 h, 12 h, 24 h, 48 h, and 72 h after treatment. The number of viable cells was quantified via a cell CCK-8 assay. Following the protocol, a CCK-8 kit was added to each well (10 µL/well) for 2 ± 0.5 h before measurement. The absorbance of the cells was measured with a microplate reader at a wavelength of 450 nm. The data were calculated by dividing the cell viability in real-time by the blank through the absorbance and proportion with various dosages of treatment.[5,34] The cell experiments were conducted with at least three times repetition.

Histological Evaluation of Key Organs Using H&E Staining

The H&E staining was used for the tissue toxicology assay. At pre-established times for biopsy up to 14 d, the kidney, liver, and stomach tissues were harvested and immediately stored in 4% PFA at 4 °C. The tissues were subsequently rinsed with 1× PBS, subjected to standard histological processing, and embedded in paraffin for sectioning (4 µm thick) was obtained before staining.[36–38] The tissue was then examined and assessed in detail via a highly accurate Nikon Eclipse E100 upright microscope, ensuring the reliability of the results.

In vivo Behavioral Assessment Using ICR Mice

Male Outbred BLTW: CD1 (ICR) mice, aged 6–8 weeks and weighing 30 ± 2 g at the start of the experiments, were used in this study. All animal procedures were carried out following the criteria of the National Cheng Kung Medical College Animal Care Committee (IACUC Approval No.: 108,170). The animal pain model was induced by administering 5 μL of CFA to each mouse. After establishing inflammatory pain, baseline behavioral assessments and withdrawal threshold measurements were performed via Dixon's up-and-down method.[39,40] The assessment of mechanical allodynia was performed with Von Frey filaments (Touch Test® Sensory Assessors, North Coast), applied to the foot via filaments with increasing logarithmic stiffness (0.02–2.56 g).[5] Following these assessments, all the experimental groups received intravenous injections of 200 μL of the prepared solutions, which contained different dosages of the free drugs and nanoparticles, under anesthesia with 1% isoflurane. After cessation of anesthesia, the mice were placed on an overhead metal grid to recover before further behavioral assessments.[41] The analgesic effects of the drugs were evaluated every 2 h to 10 h on the first day and daily until the seventh day after pain induction. We euthanized the mice after the experiment (on 7 d and 14 d) using 4% isoflurane to induce deep anesthesia, then collected the liver, kidney, stomach, and hind paw tissues for histological examination.

Immunohistochemistry Analyses

At the end of the animal behavioral experiment (8 h), the hind paw tissues were harvested and used for IHC examination. The paraffin-embedded sections (4 μm thick) were subjected to a thorough process of dewaxing and rehydration involving sequential immersion in xylene, followed by 99.9%, 95%, and 75% EtOH solutions and 1× PBS, respectively. The antigen retrieval process was performed by treating the sections with a buffer solution containing 10 mm Tris base, 1 mm EDTA, and 0.05% Tween 20, with the pH set to 9.0 in a pressure cooker for 5 min. Endogenous peroxidase activity was inhibited by incubating the sections for 10 min with 3% hydrogen peroxide, followed by blocking with a 5% FBS solution in 1× PBS for 60 min. The sections were subsequently incubated overnight at 4 °C with primary antibodies (diluted at 1:50), including anti-COX-1, anti-COX-2, and rabbit anti-PGE_2. After rinsing with PBST (1× PBS containing 0.1% Tween 20), the sections were incubated at room temperature for 2 h with a prediluted secondary antibody (1:100 dilution) — anti-rabbit HRP in blocking solution. Following another wash with PBST, the immunoreactivity of the primary antibodies was detected via DAB for 5 min. Finally, the slides were dehydrated by sequential immersion in 75% EtOH, xylene, 95% EtOH, and 99.9% EtOH, and cleared with xylene, then mounted with the Thermo Scientific DPX mounting media and covered with a glass coverslip.

Quantification and Statistics

The data were graphically visualized via GraphPad Prism, version 10.0.3 (217) software, demonstrating our comprehensive approach to data visualization. H&E images were captured through CaptaVision plus Imaging Software (v2.1) (Nikon Eclipse E100-LED Upright Microscope) and processed via a computer-assisted imaging analysis platform (ImageJ, NIH).[42] IHC images were captured and quantified via TissueFAXS, Zeiss AxioImager Z1 Microscope System (Tissue-Gnostics). All data were analyzed statistically using either a one-way analysis of variance (ANOVA) followed by Bonferroni's multiple comparisons test, or a two-way ANOVA followed by Tukey's multiple comparisons test for comparisons involving two variables ($p < 0.05$) to assess the significance between data points. All measurements were triplicated for reliability, with calibration curves and representative absorption peaks of KT and PRED shown in Supplementary Figure S1 to validate analytical accuracy. Data are presented as the mean ± standard error of the mean (SEM).

Results

Synthesis and Characterization of KT-PRED-PLGA Nanoparticles

The PLGA, KT-PLGA, and KT-PRED-PLGA nanoparticles were formulated, synthesized, and characterized by related particle size, polydispersity index (PDI), and zeta potential. According to The TEM images, the average particle size of the PLGA, KT-PLGA, and KT-PRED-PLGA nanoparticles were 147.29 ± 3.27, 170.37 ± 3.35, and 166.20 ± 7.97 nm in diameter, respectively, with a spherical shape (Figure 1A–C). Furthermore, the PDI for each type of nanoparticle was 0.17 ± 0.0013 for the PLGA, 0.25 ± 0.0128 for the KT-PLGA and 0.14 ± 0.0003 for the KT-PRED-PLGA, as measured via DLS (Figure 1D–F). The effective electric surface charge on the entrapped drug KT-PRED-PLGA was negative at −15.81 ± 0.34 mV (Figure 1G).

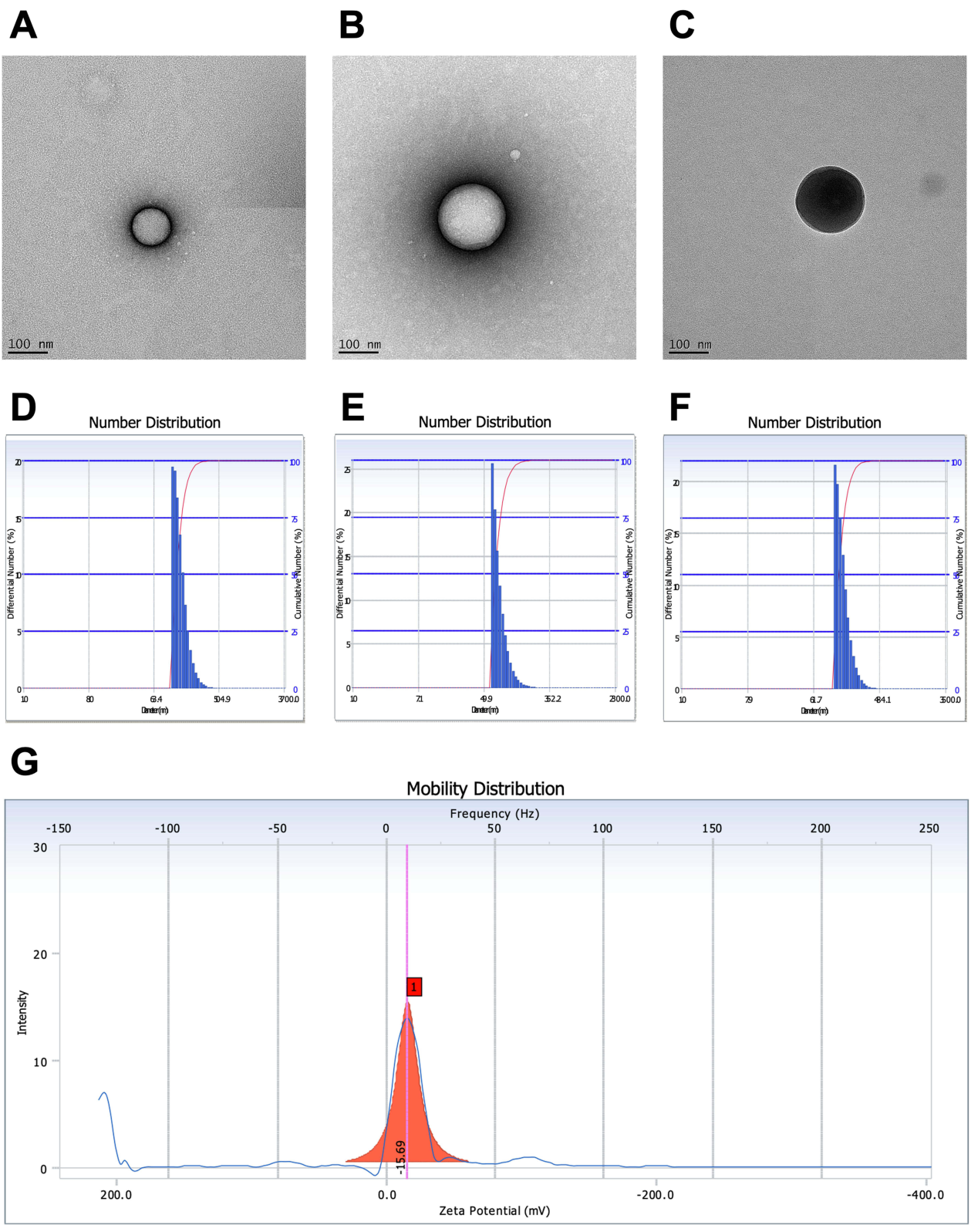

Figure 1 Characterization of the synthesized nanoparticles: nanoparticle morphology (**A-C**) via TEM, hydrodynamic size (**D-F**) of PLGA, KT-PLGA, and KT-PRED-PLGA, respectively, and zeta potential (**G**) of KT-PRED-PLGA measured by DLS. The values are presented as the mean ± SEM, n = 3 per group.

Characterization of Loading Capacity, Encapsulation Efficiency, and Drug Release Profile

The DL, EE, and DR profile of KT and PRED within PLGA nanoparticles were measured using UV-Vis spectrophotometry, with optical absorbance at 325 nm for KT and 248 nm for PRED (Figure 2). The loading capacity was >18% for both KT and PRED, and the EE exceeded 80%, >24 mg (Figure 2A). Cumulative DR (%) was monitored over 120 h, showing a release of 92.53% for KT and 81.12% for PRED on the first day (Figure 2B).

Assessment of Cellular Toxicity

Evaluating the biocompatibility of therapeutic drugs is essential for their clinical application. The cytotoxicity of both KT-PRED-PLGA nanoparticles and KT + PRED free drugs was assessed using a CCK-8 assay at different concentrations (100, 500, and 1000 μg/mL) and exposure times in Vero cells. Cell viability was measured by light absorbance at 450 nm using a microplate reader. As shown in Figure 3, both KT-PRED-PLGA nanoparticles and KT + PRED free drugs exhibited minimal toxicity across all concentrations. Notably, KT-PRED-PLGA nanoparticles were safer than KT + PRED free drugs after 72 h of continuous treatment. Over time, the KT-PRED-PLGA nanoparticles and the KT + PRED free drugs had very different effects on the viability of cells.

In Vivo Assessment of Biosafety

In addition to in vitro cell tests, an animal study was conducted to assess biosafety. Tissue samples from the liver, kidney, and stomach were collected and stained with H&E after 7 d and 14 d of treatment to observe any morphological or histological changes. On account of vulnerability scores of 0.6–1.2 on a 3-point scale, the KT-PRED-PLGA nanoparticles at low (40 mg/kg) and high (80 mg/kg) doses (Figure 4A–C) caused minimal tissue damage in the liver, kidney, and stomach, maintaining near-normal morphology over 14 d, compared with PBS and KT + PRED free drugs. In contrast, the KT + PRED free drugs resulted in substantial tissue damage (Figure 4D-F). Notably, the highest dose of KT 80 mg/kg + PRED 80 mg/kg severely damaged kidney tissue (Figure 4F). No changes were observed in the appearance or behavior of the mice.

Mechanical Allodynia Testing for Analgesic Efficacy Evaluation

The multi-dosage experiment aimed to optimize pain relief among treatment groups: PBS, KT (80 mg/kg) + PRED (8 mg/kg), KT (80 mg/kg) + PRED (80 mg/kg), and KT-PRED-PLGA nanoparticles (80 mg/kg). Highly, KT (80 mg/kg) + PRED (8 mg/kg) exhibited significant analgesia from 1 h to 4 h, peaking at 2.08 ± 0.23, then declining to 1.14 ± 0.16. After 4 h, KT-PRED-PLGA nanoparticles (80 mg/kg) in Figure 5A demonstrated increasing and sustained pain relief, peaking at 1.7 ± 0.35.

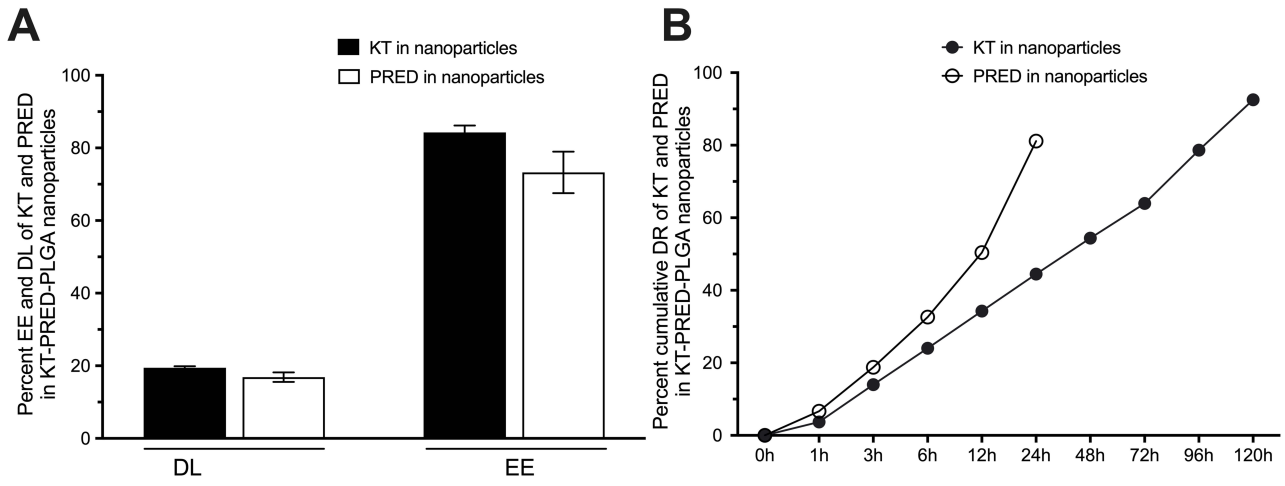

Figure 2 (**A**) EE and DR percentage (wt%) of KT and PRED inside PLGA nanoparticles. (**B**) In vitro drug release, correlation coefficients (r) for mathematical models that fit the release kinetics in HG-DMEM +20%FBS, pH 8.5. The release profiles of KT and PRED loaded PLGA nanoparticles were determined by measuring the optical absorption via UV-Vis spectrophotometry at 325 nm for KT and 248 nm for PRED. The values are presented as the mean ± SEM, n = 3 per group.

https://doi.org/10.2147/IJN.S515452

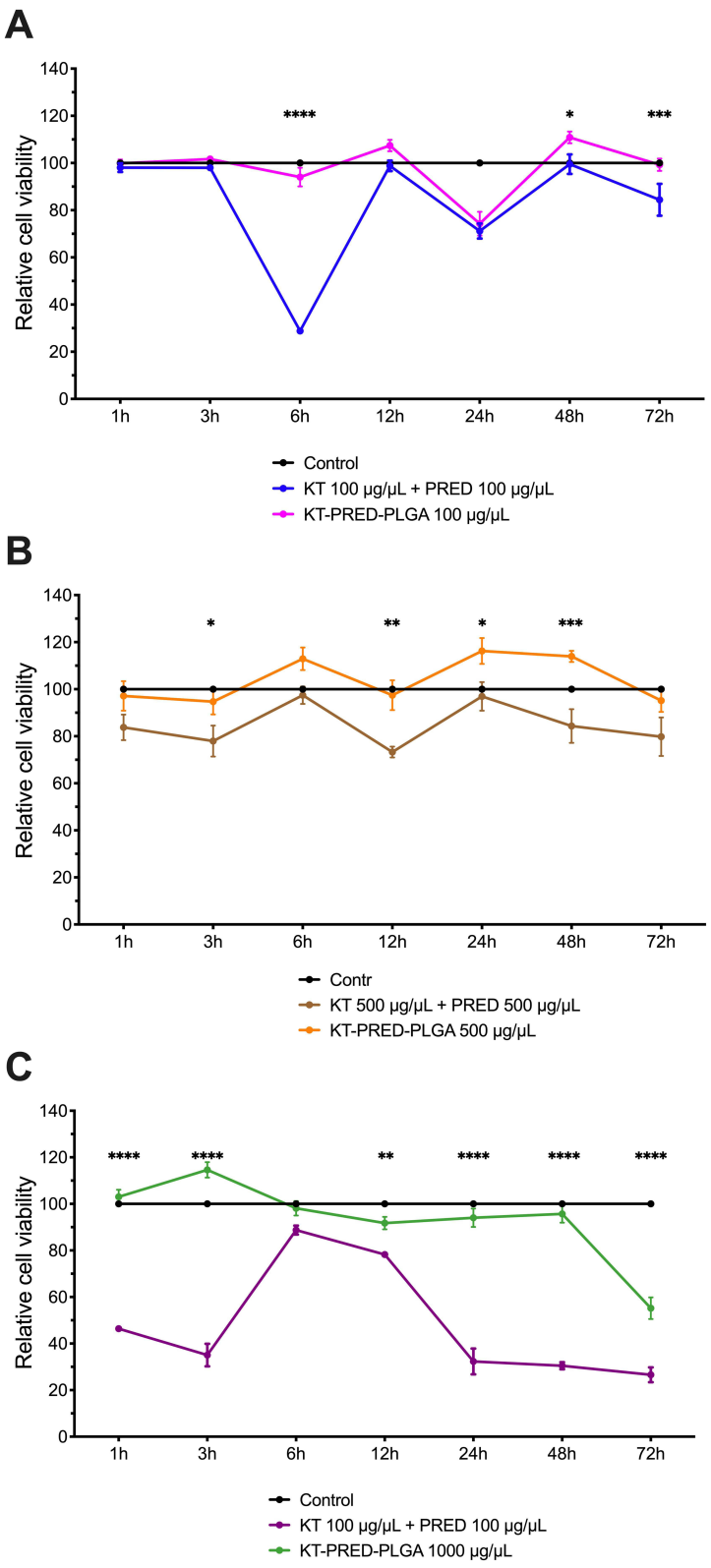

Figure 3 Cell viability of Vero cells exposed to KT + PRED free drugs and KT-PRED-PLGA nanoparticles at different concentrations over time. (**A**) 100 µg/mL, (**B**) 500 µg/mL, and (**C**) 1000 µg/mL. The CCK-8 assay was performed at 1, 3, 6, 12, 24, 48, and 72 h post-treatment. Groups: Control, KT + PRED free drugs, and KT-PRED-PLGA nanoparticles. Two-way ANOVA: *indicates $p < 0.05$, **indicates $p < 0.01$, ***indicates $p < 0.001$, and ****indicates $p < 0.0001$ versus the KT + PRED free drugs. Data are presented as mean ± SEM (n = 3).

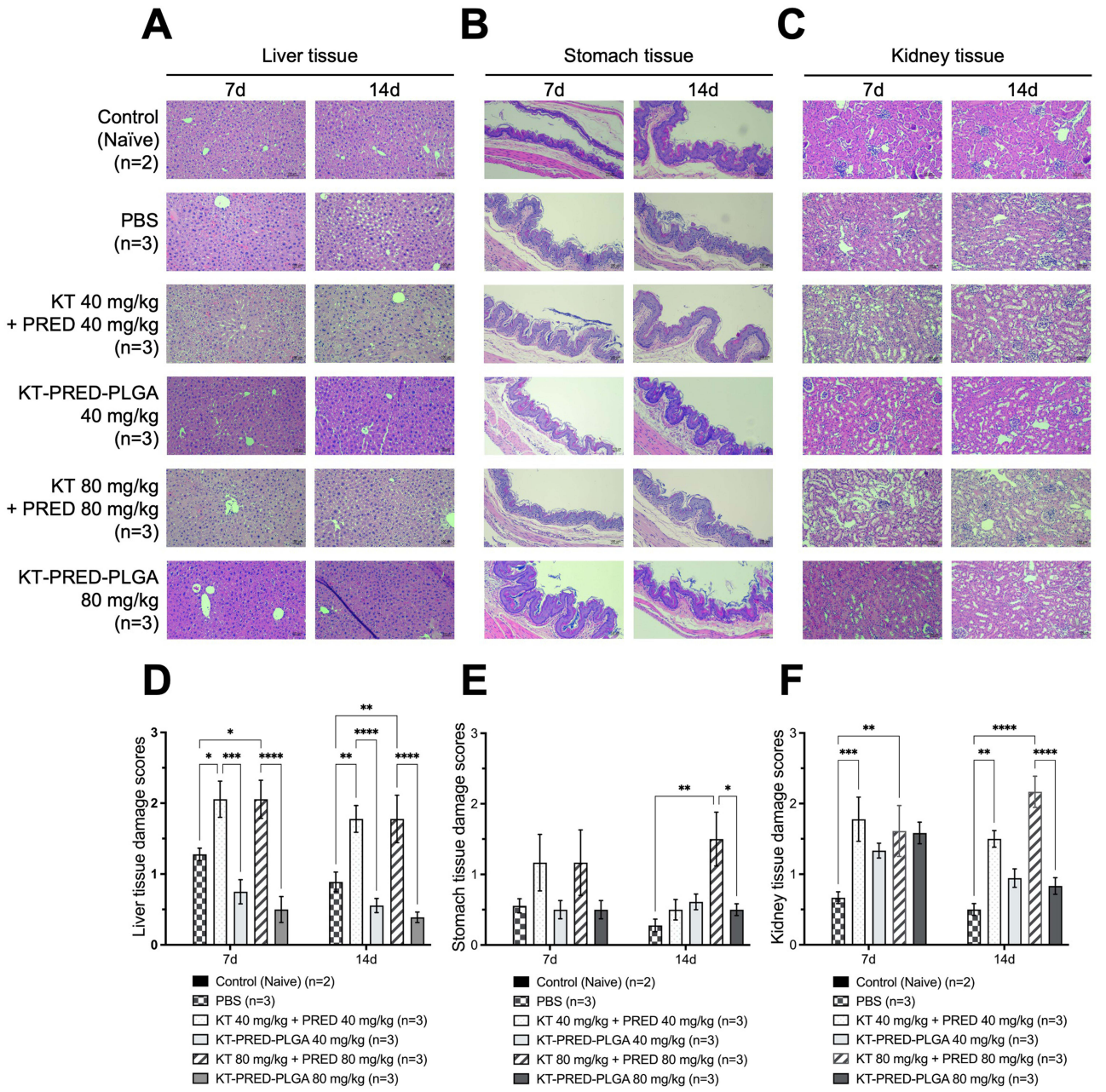

Figure 4 (**A-C**) Histological trauma intensity and proportion compared to normal tissue and (**D-F**) histological injury scores of the liver, stomach, and kidney after the indicated treatments. The injury scores were based on the level of damage intensity, including factors such as inflammation and cytoarchitectural changes. Two-way ANOVA: *indicates $p < 0.05$, **indicates $p < 0.01$, ***indicates $p < 0.001$, and ****indicates $p < 0.0001$. The values are presented as the mean ± SEM, n = 17. Scale bar = 100 μm.

Mechanical sensitivity tests using Dixon's up-and-down method confirmed that KT-PRED-PLGA nanoparticles provided consistent analgesia from 6 h to 26 h (Figure 5B), with detailed values as follows: at 6 h, PBS (1.14 ± 0.23), KT-PRED-PLGA nanoparticles (40 mg/kg) (1.48 ± 0.36), and KT-PRED-PLGA nanoparticles (80 mg/kg) (1.79 ± 0.19), and with similar results at 8 h, 10 h, and 24 h. Overall, KT-PRED-PLGA nanoparticles produced superior analgesic effects compared to free drugs.

Protein Expression Profiling in the Arachidonic Acid (AA) Pathway

IHC analysis of COX-1, COX-2, and PGE_2 protein expression in hind paw tissues revealed significant inhibition of these proteins following treatment. Immunostaining images (Figure 6A–C) and corresponding intensity scores (Figure 6D–F) illustrate these effects. The study, which included control, PBS, KT (80 mg/kg) + PRED (80 mg/kg), and KT-PRED-

https://doi.org/10.2147/IJN.S515452

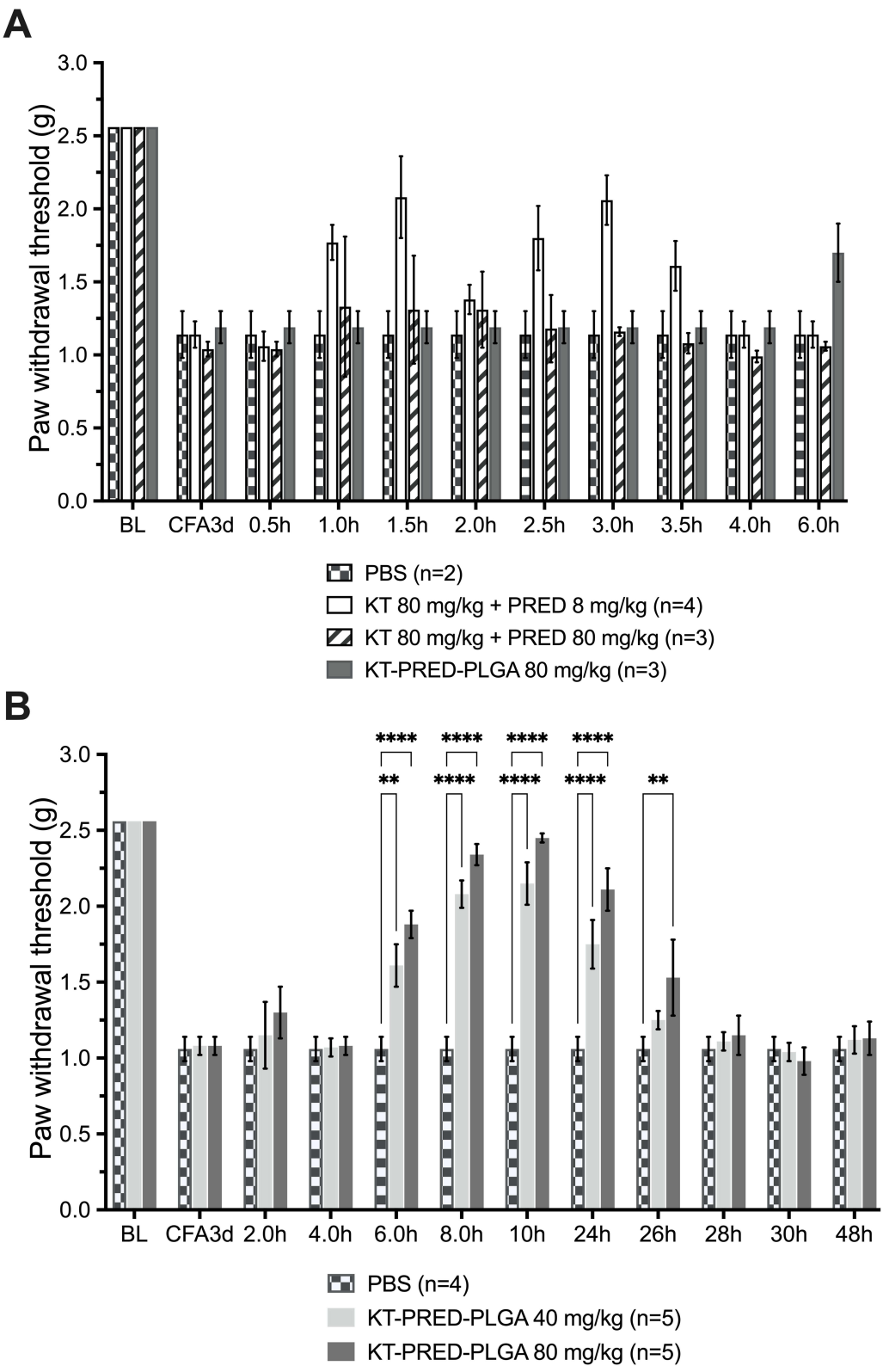

Figure 5 Mechanical pain sensitivity was measured to assess the effects of KT + PRED free drugs and KT-PRED-PLGA nanoparticles. The treatment was divided into two phases: (**A**) the initial 6 h, n = 12 and (**B**) the extended treatment period up to 48 h, n = 14. Two-way ANOVA: **indicates $p < 0.01$; ****indicates $p < 0.0001$. The values are presented as the mean ± SEM.

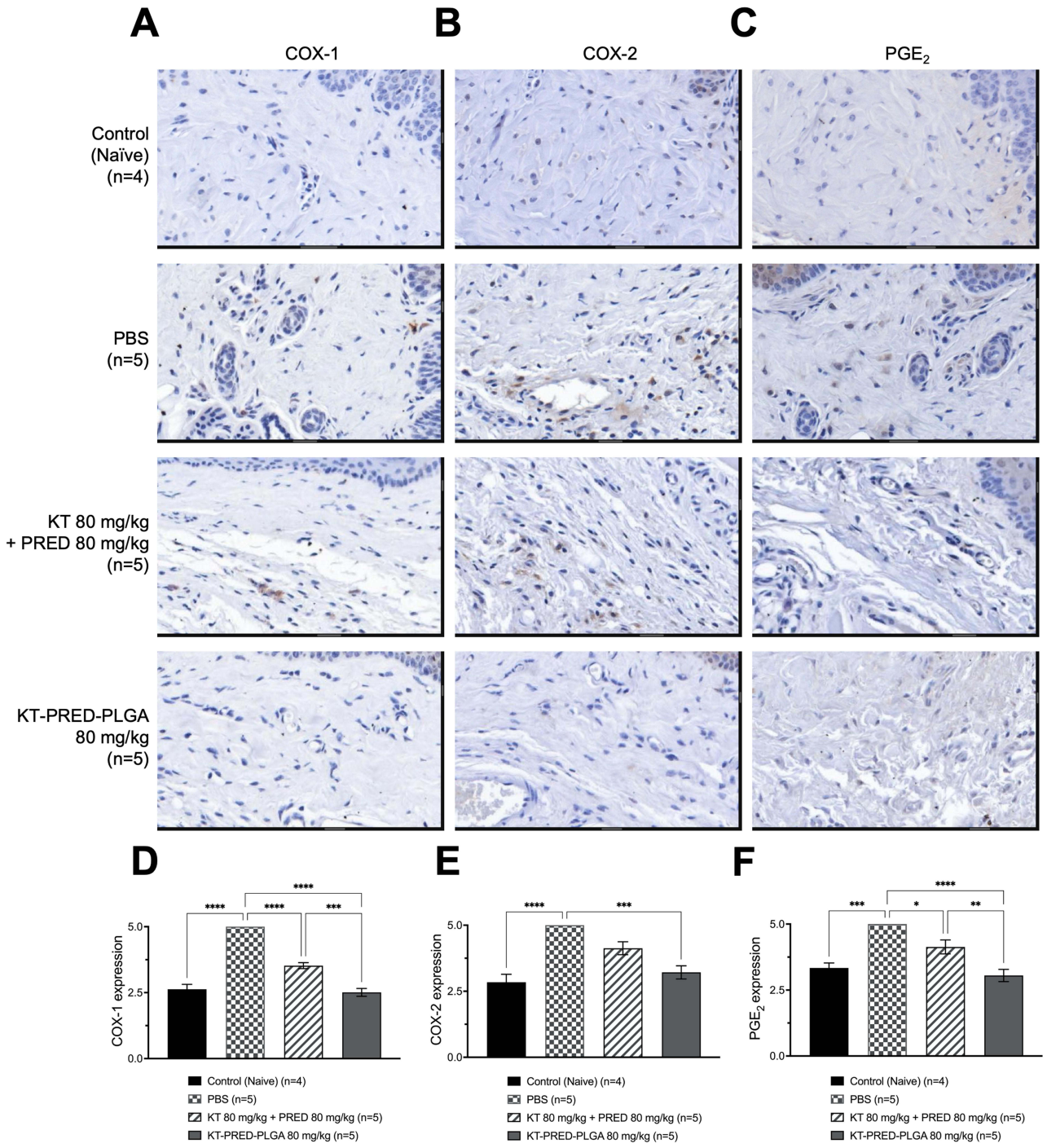

Figure 6 Immunostaining was performed to evaluate the protein expression of cyclooxygenase (COX-1), COX-2, and PGE_2. (**A-C**) Images of IHC staining samples and (**D-F**) associated intensities are presented as intensity scores for the indicated treatments. The DAB score was determined and referenced following the scoring system outlined by Klein et al. One-way ANOVA: *indicates $p < 0.05$, **indicates $p < 0.01$, ***indicates $p < 0.001$, and ****indicates $p < 0.0001$. The values are presented as the mean ± SEM, n = 19. Scale bar = 100 μm.

PLGA nanoparticles (80 mg/kg), showed high reliability. Specifically, COX-1 expression levels were 2.63 ± 0.18 in the control, 5 in PBS, 3.52 ± 0.11 in KT + PRED free drugs, and 2.51 ± 0.15 in KT-PRED-PLGA nanoparticles (Figure 6D). COX-2 levels were 2.84 ± 0.30 in the control, 5 in PBS, 4.13 ± 0.24 in KT + PRED free drugs, and 3.26 ± 0.25 in KT-PRED-PLGA nanoparticles (Figure 6E). PGE_2 levels were 3.34 ± 0.19 in the control, 5 in PBS, 4.13 ± 0.26 in KT + PRED, and 3.05 ± 0.23 in KT-PRED-PLGA nanoparticles (Figure 6F).

https://doi.org/10.2147/IJN.S515452

Discussion

The double-emulsion (W/O/W) technique was selected in this study to address a central challenge in dual-drug delivery: the co-encapsulation of hydrophilic and hydrophobic compounds with controlled release. This approach is widely recognized for enhancing drug loading efficiency and achieving sustained delivery, especially in polymer-based nanocarriers.[43] Compared to single-emulsion or co-administration strategies, W/O/W systems provide compartmentalized loading and precise modulation of release profiles.[44,45] These features are particularly beneficial in chronic pain management, where maintaining therapeutic drug levels while minimizing side effects is essential.[9,46,47]

The co-encapsulation of KT and PRED within a single PLGA nanoparticle leverages the complementary pharmacological actions of each drug. PRED, a corticosteroid, provides rapid anti-inflammatory and immunomodulatory effects, while KT, an NSAID, offers sustained analgesic and anti-inflammatory action.[45,46,48] Their combined release from a single matrix enables both immediate and sustained control of inflammation. Although prior studies have investigated each drug individually in PLGA carriers,[9,10] the integration of both agents within a unified nanoplatform remains underexplored.[26,41] Moreover, the KT-PRED-PLGA nanoparticles had a low PDI of less than 0.2, which means they are all about the same size, helping to release the drug steadily and enhances in vivo performance.[49] Additionally, their moderately negative zeta potential supports excellent colloidal stability and minimizes nonspecific cellular interactions, both of which are advantageous for systemic administration and therapeutic efficacy.[49,50]

Notably, our formulation strategy aligns with emerging evidence supporting the therapeutic benefits of nanocarrier-enabled combinatorial drug delivery systems. Previous investigations have shown that such systems can reduce overall dosing frequency and mitigate systemic toxicity.[11,31] In our study, the minimized tissue damage and acceptable cytocompatibility observed suggest that the nanoparticle matrix effectively buffers local drug concentrations and limits off-target effects.[18,20] These results reinforce the protective role of PLGA as both a sustained-release system and a biocompatible carrier.

Beyond formulation advantages, the therapeutic mechanism is further supported by molecular evidence. Tests indicated that KT-PRED-PLGA nanoparticles reduce important substances that cause inflammation in the AA pathway, such as COX-1, COX-2,[51] and PGE_2.[4,26,52,53] This pathway plays a pivotal role in chronic inflammatory conditions,[51,54] and dual inhibition at both enzymatic and downstream levels has been associated with enhanced therapeutic efficacy.[53,55–57] The 8 h timepoint for IHC analysis was selected based on the observed onset and stabilization of the analgesic effect of KT-PRED-PLGA nanoparticles. At this time, the KT-PRED-PLGA NPs 80 mg/kg exhibited significantly enhanced analgesia compared to the KT 80 mg/kg + PRED 80 mg/kg (Two-way ANOVA, $p < 0.0001$), as illustrated in Supplementary Figure S2. This behavioral improvement corresponded with a pronounced reduction in COX-1, COX-2, and PGE_2 expression, confirming the formulation's effective anti-inflammatory action at the protein level. By simultaneously suppressing multiple pro-inflammatory targets, the nanoparticles achieve a broader and more coordinated regulation of the inflammatory cascade than free-drug administration alone.

Conclusion

In this study, we demonstrated the successful application of a double-emulsion method for formulating PLGA nanoparticles capable of co-delivering hydrophilic and hydrophobic drugs with sustained release and favorable biocompatibility. The KT-PRED-PLGA nanoparticles provide clear benefits for treatment, such as better pain relief, less harm to tissues, and greater safety than traditional methods. Its capacity to modulate key inflammatory pathways further supports its utility in chronic pain management. These findings highlight the formulation's promise as a safer and more effective nanotherapeutic platform. Future investigations should explore its clinical translation, large-scale production, and application in broader inflammatory or pain-related conditions.

Ethics Approval and Informed Consent

The animal studies were performed according to the National Cheng Kung Medical College Animal Care Guidelines (IACUC approval No: 108170).

Consent for Publication

All the authors have reviewed all the manuscripts and stated that the manuscript has no significant part of it under consideration elsewhere.

Acknowledgments

This work was supported by the Center of Applied Nanomedicine (CAN) and Medical Device Innovation Center (MDIC) at National Cheng Kung University (NCKU), through the Featured Areas Research Center Program under the Higher Education Sprout Project of the Ministry of Education (MOE), Taiwan, and by the National Science and Technology Council (NSTC), Taiwan. We acknowledge the technical assistance of the Taiwan Cryo-EM Consortium, National Core Facility for Biopharmaceuticals, NSTC, Taiwan; the University Center of Bioscience and Biotechnology at NCKU; and the Instrument Development Center at NCKU. The Bioimaging Core Facility at NCKU provided support for TissueQuest software. The graphical abstract was created using BioRender.com.

Author Contributions

All authors made a significant contribution to the work reported, whether that is in the conception, study design, execution, acquisition of data, analysis and interpretation, or in all these areas; took part in drafting, revising or critically reviewing the article; gave final approval of the version to be published; have agreed on the journal to which the article has been submitted; and agree to be accountable for all aspects of the work.

Funding

This work was supported by the Center of Applied Nanomedicine (CAN) and the Medical Device Innovation Center (MDIC) at National Cheng Kung University (NCKU) through the Featured Areas Research Center Program under the Higher Education Sprout Project of the Ministry of Education (MOE), Taiwan, and by the National Science and Technology Council (NSTC), Taiwan (grant numbers: NSTC-113-2640-B-006-002-, NSTC-112-2314-B-006-032-MY3, and MOST-108-2314-B-006-053-).

Disclosure

The authors declare that there is no conflict of interest related to this manuscript.

References

1. Raja SN, Carr DB, Cohen M, et al. The revised international association for the study of pain definition of pain: concepts, challenges, and compromises. *Pain*. 2020;161(9):1976—1982. doi:10.1097/j.pain.0000000000001939
2. Carr D, Schatman M. Cannabis for chronic pain: not ready for prime time. *Am J Public Health*. 2019;109(1):50—51. doi:10.2105/AJPH.2018.304593
3. Barakzoy AS, Moss AH. Efficacy of the World Health Organization analgesic ladder to treat pain in end-stage renal disease. *J Am Soc Nephrol*. 2006;17(11):3198—3203. doi:10.1681/ASN.2006050477
4. Brune K, Patrignani P. New insights into the use of currently available non-steroidal anti-inflammatory drugs. *J Pain Res*. 2015;8:105—118. doi:10.2147/JPR.S75160
5. Bhadelia A, De Lima L, Arreola-Ornelas H, Kwete XJ, Rodriguez NM, Knaul FM. Solving the global crisis in access to pain relief: lessons from country actions. *Am J Public Health*. 2019;109(1):58—60. doi:10.2105/AJPH.2018.304769
6. Kowalski ML, Asero R, Bavbek S, et al. Classification and practical approach to the diagnosis and management of hypersensitivity to nonsteroidal anti-inflammatory drugs. *Allergy*. 2013;68(10):1219—1232. doi:10.1111/all.12260
7. Litvak KM, McEvoy GK. Ketorolac, an injectable nonnarcotic analgesic. *Clin Pharm*. 1990;9(12):921—935. doi:10.1093/ajhp/48.1.168
8. Ho ML, Chang JK, Wang GJ. Effects of ketorolac on bone repair: a radiographic study in modeled demineralized bone matrix grafted rabbits. *Pharmacology*. 1998;57(3):148—159. doi:10.1159/000028236
9. Khaled KA, Sarhan HA, Ibrahim MA, Ali AH, Naguib YW. Prednisolone-loaded PLGA microspheres. In vitro characterization and in vivo application in adjuvant-induced arthritis in mice. *AAPS Pharm Sci Tech*. 2010;11(2):859—869. doi:10.1208/s12249-010-9445-5
10. Giovagnoli S, Blasi P, Ricci M, Schoubben A, Perioli L, Rossi C. Physicochemical characterization and release mechanism of a novel prednisone biodegradable microsphere formulation. *J Pharm Sci*. 2008;97(1):303—317. doi:10.1002/jps.21073
11. Fargnoli AS, Mu A, Katz MG, et al. Anti-inflammatory loaded poly-lactic glycolic acid nanoparticle formulations to enhance myocardial gene transfer: an in-vitro assessment of a drug/gene combination therapeutic approach for direct injection. *J Transl Med*. 2014;12(1):1—9. doi:10.1186/1479-5876-12-171
12. Brown CR, Moodie JE, Dickie G, et al. Analgesic efficacy and safety of single-dose oral and intramuscular ketorolac tromethamine for postoperative pain. *Pharmacotherapy*. 1990;10(6P2):59S—70S. doi:10.1002/j.1875-9114.1990.tb03582.x

13. Simone JN, Pendelton RA, Jenkins JE. Comparison of the efficacy and safety of ketorolac tromethamine 0.5% and prednisolone acetate 1% after cataract surgery. *J Cataract Refract Surg*. 1999;25(5):699–704. doi:10.1016/S0886-3350(99)00023-1
14. Perry HD, Donnenfeld ED. An update on the use of ophthalmic ketorolac tromethamine 0.4%. *Expert Opin Pharmacother*. 2006;7(1):99–107. doi:10.1517/14656566.7.1.99
15. Zeb A, Gul M, Nguyen TTL, Maeng HJ. Controlled release and targeted drug delivery with poly(lactic-co-glycolic acid) nanoparticles: reviewing two decades of research. *J Pharm Investig*. 2022;52(6):683–724. doi:10.1007/s40005-022-00584-w
16. Phm TL, Kim DW. Poly(lactic-co-glycolic acid) nanomaterial-based treatment options for pain management: a review. *Nanomedicine*. 2020;15(19). doi:10.2217/nnm-2020-0114
17. Bohrey S, Chourasiya V, Pandey A. Polymeric nanoparticles containing diazepam: preparation, optimization, characterization, in-vitro drug release and release kinetic study. *Nano Converg*. 2016;3(1):3. doi:10.1186/s40580-016-0061-2
18. Te Boekhorst BCM, Jensen LB, Colombo S, et al. MRI-assessed therapeutic effects of locally administered PLGA nanoparticles loaded with anti-inflammatory siRNA in a murine arthritis model. *J Control Release*. 2012;161(3):772—780. doi:10.1016/j.jconrel.2012.05.004
19. Mundargi RC, Babu VR, Rangaswamy V, Patel P, Aminabhavi TM. Nano/micro technologies for delivering macromolecular therapeutics using poly(d, l-lactide-co-glycolide) and its derivatives. *J Control Release*. 2008;125(3):193—209. doi:10.1016/j.jconrel.2007.09.013
20. Wang X, Wang S, Zhang Y. Advance of the application of nano-controlled release system in ophthalmic drug delivery. *Drug Deliv*. 2016;23 (8):2897—2901. doi:10.3109/10717544.2015.1116025
21. Zhu Z, Li Y, Yang X, Pan W, Pan H. The reversion of anti-cancer drug antagonism of tamoxifen and docetaxel by the hyaluronic acid-decorated polymeric nanoparticles. *Pharmacol Res*. 2017;126:84—96. doi:10.1016/j.phrs.2017.07.011
22. Brocks DR, Jamali F. Clinical Pharmacokinetics of Ketorolac Tromethamine. *Clin Pharmacokinet*. 1992;23(6):415—427. doi:10.2165/00003088-199223060-00003
23. Massó González EL, Patrignani P, Tacconelli S, García Rodríguez LA. Variability among nonsteroidal antiinflammatory drugs in risk of upper gastrointestinal bleeding. *Arthritis Rheum*. 2010;62(6):1592—1601. doi:10.1002/art.27412
24. Kawabata A. Prostaglandin E2 and pain - An update. *Biol Pharm Bull*. 2011;34(8):1170—1173. doi:10.1248/bpb.34.1170
25. Yu T, Lao X, Zheng H. Influencing COX-2 activity by COX related pathways in inflammation and cancer. *Mini-Rev Med Chem*. 2016;16 (15):1230—1243. doi:10.2174/1389557516666160505115743
26. Ali KA, Maity A, Roy SD, Das Pramanik S, Pratim Das P, Shaharyar MA. Insight into the mechanism of steroidal and non-steroidal anti-inflammatory drugs. In: *How Synthetic Drugs Work: Insights Into Molecular Pharmacology of Classic and New Pharmaceuticals*. Academic Press; 2023:61—94. doi:10.1016/B978-0-323-99855-0.00004-X
27. Praveen Rao PN, Knaus EE. Evolution of nonsteroidal anti-inflammatory drugs (NSAIDs): cyclooxygenase (COX) inhibition and beyond. *J Pharm Pharm Sci*. 2008;11(2):81s—110s. doi:10.18433/j3t886
28. Mahesh G, Kumar KA, Reddanna P. Overview on the discovery and development of anti-inflammatory drugs: should the focus be on synthesis or degradation of PGE2? *J Inflamm Res*. 2021;14:253—263. doi:10.2147/JIR.S278514
29. Floyd JA, Galperin A, Ratner BD. Drug encapsulated aerosolized microspheres as a biodegradable, intelligent glioma therapy. *J Biomed Mater Res A*. 2016;104(2):544—552. doi:10.1002/jbm.a.35547
30. Wei B, Cai C, Tian Y. Nano-sized starch: preparations and applications. In: Jin Z, editor. *Functional Starch and Applications in Food*. Singapore: Springer; 2018:147—176. doi:10.1007/978-981-13-1077-5
31. Danhier F, Ansorena E, Silva JM, Coco R, Le Breton A, Préat V. PLGA-based nanoparticles: an overview of biomedical applications. *J Control Release*. 2012;161(2):505—522. doi:10.1016/j.jconrel.2012.01.043
32. Wagh D, Pothineni VR, Inayathullah M, Liu S, Kim KM, Rajadas J. Borreliacidal activity of Borrelia metal transporter A (BmtA) binding small molecules by manganese transport inhibition. *Drug Des Devel Ther*. 2015;9:805—816. doi:10.2147/DDDT.S77063
33. Lau AKS, Wong TTW, Ho KK, et al. Interferometric time-stretch microscopy for ultrafast quantitative cellular and tissue imaging at 1 μm. *J Biomed Opt*. 2014;19(7):1—7. doi:10.1117/1.jbo.19.7.076001
34. Saini N, Mathur R, Agrawal SS. Qualitative and quantitative assessment of four marketed formulations of Brahmi. *Indian J Pharm Sci*. 2012;74 (1):24. doi:10.4103/0250-474X.102539
35. Bian YY, Guo J, Zhu KX, Guo XN, Peng W, Zhou HM. Resistance investigation of wheat bran polyphenols extracts on HEK293 cells against oxidative damage. *RSC Adv*. 2015;5(21):16116—16124. doi:10.1039/c4ra13602k
36. Thoolen B, Maronpot RR, Harada T, et al. Proliferative and nonproliferative lesions of the rat and mouse hepatobiliary system. *Toxicol Pathol*. 2010;38(7 Suppl):5S—81S. doi:10.1177/0192623310386499
37. Clatworthy MR, Kettunen MI, Hu DE, et al. Magnetic resonance imaging with hyperpolarized [1, 4-13C2] fumarate allows detection of early renal acute tubular necrosis. *Proc Natl Acad Sci*. 2012;109(33):13374—13379. doi:10.1073/pnas.1205539109
38. Nolte T, Brander-Weber P, Dangler C, et al. Nonproliferative and proliferative lesions of the gastrointestinal tract, pancreas and salivary glands of the rat and mouse. *J Toxicol Pathol*. 2016;29(1 Suppl):1S—125S. doi:10.1293/tox.29.1S
39. Kim JE, Nam JH, Cho JY, Kim KS, Hwang DY. Annual tendency of research papers used ICR mice as experimental animals in biomedical research fields. *Lab Anim Res*. 2017;33(2):171—174. doi:10.5625/lar.2017.33.2.171
40. Gould TD, Einat H. Animal models of bipolar disorder and mood stabilizer efficacy: a critical need for improvement. *Neurosci Biobehav Rev*. 2007;31(6):825—831. doi:10.1016/j.neubiorev.2007.05.007
41. Ho KY, Gwee KA, Cheng YK, Yoon KH, Hee HT, Omar AR. Nonsteroidal anti-inflammatory drugs in chronic pain: implications of new data for clinical practice. *J Pain Res*. 2018;11:1937—1948. doi:10.2147/JPR.S168188
42. Gurcan MN, Boucheron LE, Can A, Madabhushi A, Rajpoot NM, Yener B. Histopathological image analysis: a review. *IEEE Rev Biomed Eng*. 2009;2:147—171. doi:10.1109/RBME.2009.2034865
43. Iqbal M, Zafar N, Fessi H, Elaissari A. Double emulsion solvent evaporation techniques used for drug encapsulation. *Int J Pharm*. 2015;496 (2):173—190. doi:10.1016/j.ijpharm.2015.10.057
44. Chirag N, Narendra C, Sandip P, Upendra P, Keyur A, Dhruti N. Design and characterization of bioadhesive microspheres prepared by double emulsion solvent evaporation method. *Acta Pharma Sci*. 2009;51(3):261—270.
45. Vadivelu N, Gowda AM, Urman RD, et al. Ketorolac tromethamine - Routes and clinical implications. *Pain Pract*. 2015;15(2):175—193. doi:10.1111/papr.12198

46. Araújo J, Gonzalez E, Egea MA, Garcia ML, Souto EB. Nanomedicines for ocular NSAIDs: safety on drug delivery. *Nanomedicine*. 2009;5(4):394—401. doi:10.1016/j.nano.2009.02.003
47. Sinha VR, Trehan A. Formulation, characterization, and evaluation of ketorolac tromethamine-loaded biodegradable microspheres. *Drug Delivery*. 2005;12(3):133—139. doi:10.1080/10717540590925726
48. Sinha VR, Kumar RV, Singh G. Ketorolac tromethamine formulations: an overview. *Expert Opin Drug Deliv*. 2009;6(9):961—975. doi:10.1517/17425240903116006
49. Danaei M, Dehghankhold M, Ataei S, et al. Impact of particle size and polydispersity index on the clinical applications of lipidic nanocarrier systems. *Pharmaceutics*. 2018;10(2):57. doi:10.3390/pharmaceutics10020057
50. Zhang HH, Kuo WS, Tu PY, et al. Enhancing lung recovery: inhaled poly(lactic-co-glycolic) acid encapsulating FTY720 and nobiletin for lipopolysaccharide-induced lung injury, with advanced inhalation tower technology. *ACS Nano*. 2025;19(8):7634–7649. doi:10.1021/acsnano.3c12532
51. Wu PC, Bin SD, Hsiao HT, Wang JCF, Lin YC, Liu YC. Magnetic field distribution modulation of intrathecal delivered ketorolac iron-oxide nanoparticle conjugates produce excellent analgesia for chronic inflammatory pain. *J Nanobiotechnology*. 2018;16(1). doi:10.1186/s12951-018-0375-9
52. Wang B, Wu L, Chen J, et al. Metabolism pathways of arachidonic acids: mechanisms and potential therapeutic targets. *Signal Transduct Target Ther*. 2021;6(1):94. doi:10.1038/s41392-020-00443-w
53. Ahmadi M, Bekeschus S, Weltmann KD, von Woedtke T, Wende K. Non-steroidal anti-inflammatory drugs: recent advances in the use of synthetic COX-2 inhibitors. *RSC Med Chem*. 2022;13:471—496. doi:10.1039/d1md00280e
54. Wu PC, Hsiao HT, Lin YC, Bin SD, Liu YC. The analgesia efficiency of ultrasmall magnetic iron oxide nanoparticles in mice chronic inflammatory pain model. *Nanomedicine*. 2017;13(6):1975–1981. doi:10.1016/j.nano.2017.05.005
55. Meta IF, Bermolen M, MacChi R, Aguilar J. Randomized controlled trial comparing the effects of 2 analgesic drug protocols in patients who received 5 dental implants. *Implant Dent*. 2017;26(3):412—416. doi:10.1097/ID.0000000000000544
56. Warner TD, Giuliano F, Vojnovic I, Bukasa A, Mitchell JA, Vane JR. Nonsteroid drug selectivities for cyclo-oxygenase-1 rather than cyclo-oxygenase-2 are associated with human gastrointestinal toxicity: a full in vitro analysis. *Proc Natl Acad Sci U S A*. 1999;96(13):7563—7568. doi:10.1073/pnas.96.13.7563
57. Gordon SM, Brahim JS, Rowan J, Kent A, Dionne RA. Peripheral prostanoid levels and nonsteroidal anti-inflammatory drug analgesia: replicate clinical trials in a tissue injury model. *Clin Pharmacol Ther*. 2002;72(2):175—183. doi:10.1067/mcp.2002.126501